Downscaling and modelling of an ion-exchange chromatography column for purifying glucose solutions

by

Viktor Geraldsson

Department of Chemical Engineering
Lund University

June 2020

Supervisor: **Matthias Josef Beier**
Co-supervisor: **Anton Löfgren**
Examiner: **Christian Hulteberg**

Postal address
Sölvegatan 39
223 62 Lund
Email
Kem15vge@student.lu.se

Visiting address
Getingevägen 60
223 62 Lund, Sweden

Telephone
+46 73 43 44 233

Abstract

To utilize sugars as a feedstock for renewable industries, the feedstock often needs to be very pure. This is due to ionic species contaminating the sugar feedstock being potent catalyst poisons in many cases. To remove ionic species from the sugar feedstock, it is dissolved and purified using packed ion-exchange columns. In this report, a lab-scale setup of a large scale ion-exchange setup was constructed. The system was then modelled using Matlab. The goal was to produce a lab-scale setup that in theory operates similarly to the large setup and develop a model that can predict the behaviour of the system. The feed sugar content was varied using glucose, the range of glucose concentrations tested were 0, 10, 30, and 50 wt% glucose. The feed linear flow velocity was also varied, the flows studied were 0.65, 1.3 and 2.6 m/h respectively.

To simulate the kinetics of adsorption of ionic species to the resin, the equilibrium adsorption isotherm was measured experimentally. Both the temperature effect and the effect of different glucose concentrations in the liquid was studied. It was found that lower temperatures favoured the resin performance at higher glucose temperatures and higher glucose concentration had a negative effect on the resin performance.

As the isotherm had been determined for the different glucose concentrations, experimental data of the lab-scale setup was compared to model simulations. The model shows promise in emulating the experimental setup. The experimental setup does however need more work to raise reproducibility of the setup which has been a major issue throughout.

För att använda socker som förnybar råvara för kemiindustri behöver sockret ofta vara mycket rent. Detta är på grund av att salter och andra orenheter i sockret ofta är mycket starka katalysatorgift. För att rena sockret från salter löses det upp och renas med jonbytarkromatografi. I denna rapport konstrueras en labbskalad variant av en existerande storskalig jonbytarkollon. Processen simulerades även med hjälp av Matlab. Målet var att producera en enhet på labbskala som i teorin producerar jämförbara resultat som den storskaliga enheten och sedan utveckla en modell som kan förutspå hur systemet beter sig. Sockerinnehållet hos den ingående lösningen varierades med intervallen 0, 10, 30 och 50 vikts% glukos. Den linjära flödeshastigheten genom kolonnen varierades också med intervall 0.65, 1.3 och 2.6 m/h.

För att simulera adsorptionskinetiken hos packningsmaterialet bestämdes adsorptionsisotermen experimentell. Isotermen bestämdes för 0, 10, 30 och 50 vikts% glukos i vätskan samt för temperaturerna 65, 75 och 85 °C. Packningsmaterialet visade sjunkande absorptionsförmåga vid ökande glukoshalter i vätskan och även sjunkande absorptionsförmåga vid högre temperaturer.

När adsorptionsisotermen bestämts för glukos- och temperaturspannet som skulle studeras jämfördes simuleringsdata från modellen med resultat från labbuppsättningen. Modellen visade goda möjligheter i att simulera resultat från labbuppsättningen. Labbuppsättningen behöver dock mer arbete för att öka dess tillförlitlighet som varit ett problem under projektets gång.

Foreword

This master's thesis was performed in collaboration between Lund University, Faculty of Engineering and Haldor Topsoe A/S in Kgs. Lyngby. Approximately 60 percent of the assignment was performed at Haldor Topsoes A/S facilities in Kgs. Lyngby before moving equipment to Lund to continue with experiments after shutting down due to the corona pandemic.

The assignment was performed to yield a better understanding of an ion-exchange processes, particularly ion-exchange to purify glucose solutions. Using sugars like glucose is an attractive option as feedstock for renewable industries but bulk sugar is often contaminated by salts left from fertilizers. These salt contaminants are often potent catalyst poisons which can render a process economically infeasible if the catalyst is spent too fast. The focus of this assignment is, therefore, to study the dynamics and process of ion-exchange of glucose solutions to see how certain parameters like temperature and linear flow velocity affects the process. A model for the system was constructed in Matlab, where the process can be simulated under varying conditions.

I want to thank my supervisor at Haldor Topsoe, Matthias Josef Beier for all the expertise and help to perform the experimental part of the assignment as well as provide understanding in the subject. I also want to thank Christian Hulteberg for giving me this opportunity to do my thesis at Haldor Topsoe, as well as giving sound advice over the course of the project. Finally, I want to thank Anton Löfgren for his help in modelling the ion-exchange process among other things.

Contents

1 Introduction

The strive to find new reaction pathways to platform chemicals from renewable feedstocks in the chemical industry is growing as the demand for renewability and sustainability continues to increase. The supply of saccharides is high due to their overwhelming prevalence in many industries and is, therefore, an optimal feedstock for the chemical industry from an economic viewpoint.

Saccharides available today contain many ionic impurities and particles that do not pose a problem to food industries but is a large problem in the chemical industry. Ionic species present in bulk sugar like sodium- (Na^+), potassium- (K^+), calcium- (Ca^+), and chloride- (Cl^-) ions are often potent catalyst poisons and can make a process economically unfeasible by containing only 50 ppm of chloride ions for example.

1.1 Aim

The aim of this thesis is to construct a functioning lab-scale setup for purifying glucose solutions using ion-exchange chromatography, study the effects of glucose concentration and linear flow velocity on the dynamics of the system and develop a model that can successfully predict the behaviour of the system. The lab-scale setup should also, in theory, be representable of a large scale process unit present at Haldor Topsoe A/S in Kgs. Lyngby. Can a lab-scale process for ion-exchange of glucose solutions be constructed and operated functionally and can this process be successfully modelled using Matlab?

1.2 Disposition

The layout of this report is the standard layout of introduction, theory, method, results and discussion, and finally conclusion. References and appendix are also present at the end of the report. The theory section below should give the reader an understanding of ion-exchange resin structure, principle of function and driving forces of ion exchange. Furthermore, an overview of mass transfer in ion-exchange chromatography and process scaling will be given. Following the theory chapter, the method will describe the construction of the model, describing the flow of information through the different files and equations used to simulate the system. The method section also describes the experimental setup and execution of experiments, both for batch experiments determining the equilibrium isotherm of the resin and the experiments using the lab-scale chromatography column setup. Following the method is the results and discussion chapter where the equilibrium isotherm for different glucose concentrations and temperatures are presented and discussed. Experimental results from the lab-scale column as well as model data are also presented and discussed in this section. Lastly, the conclusion is presented where the problem posed in the aim is answered, central findings of the report are lifted, and further work is discussed.

2 Theory

To accomplish the task of producing a lab-scale model, several areas of theory must be covered. These areas are mass transport in chromatography columns, both external and internal mass transfer, ion-exchange resins and process scaling. These areas will each be reviewed and have their section in the theory chapter of this literature study.

2.1 Ion-exchange processes

There are many different types of ion-exchange resins. Ion-exchange resins are divided into groups after what type of ionic specie they exchange, for example, a strong acid cation resin exchange positively charged ions present on the resin with positively charged ions in the liquid. In the same vein, strong base anion resins exchange negatively charged anions present on the resin with negatively charged anions in the liquid. In this report, the focus will be on studying the behaviour of a strong acid cation resin when purifying glucose solutions of potassium ions.

Ion-exchange resins consist of beads with a porous structure with fixed co-ions dispersed over the surfaces. These fixed coins can adsorb and desorb ionic species at certain conditions. The function of the ion-exchange resin is to exchange the ions in the solution in contact with the resin with its own adsorbed ions fixed on the co-ion sites. Take, for example, a strong acid cation-exchanger where the fixed co-ion is hydrated sulfonic acid ($SO3^-H^+$). Here the fixed co-ion is sulphite ($SO3^-$), and the adsorbed ion is a hydronium ion (H^+). Now if this resin is exposed to a solution which contains another cation than H^+, let's say a sodium ion (Na^+), some of the H^+ species would desorb from their fixed co-ions and Na^+ would be adsorbed instead. *Figure 1*.

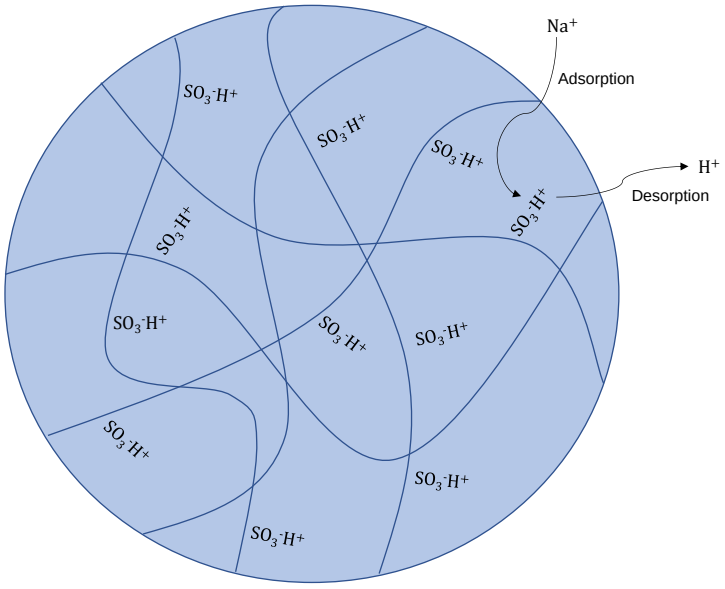

Figure 1: Shows an illustration of the structure of an ion-exchange resin with SO_3^- functional groups/ fixed co-ions and H^+ adsorbed ionic species.

Ion-exchange can be further visualized with the reaction shown below. In this typical ion-exchange reaction, R is the inert structure of the resin which is directly linked to the fixed co-ion. The line above the symbols indicates that it is in the solid phase. Here H^+ is adsorbed to the fixed co-ion (SO^-_3) initially before being desorbed and subsequently replaced by Na^+ in an adsorption/desorption equilibrium process. Observe that Cl- does not influence this reaction.

$$\overline{(R-SO_3^-)H^+} + Na^+_{(aq)} + Cl^-_{(aq)} \leftrightharpoons \overline{(R-SO_3^-)Na^+} + H^+_{(aq)} + Cl^-_{(aq)} \quad \text{(Reaction 1)}$$

Reaction 1: Shows a simple adsorption/ desorption reaction between a fixed co-ion and ionic species. R symbolizes the inert resin structure which fixes the co-ion (sulfonic acid) in place. H^+ and Na^+ are cations involved in the ion-exchange process.

The structure of ion-exchange resins can vary greatly. Many resins have a macroporous structure. Macroporous resins consist of beads in the range of typically 0.2 – 1.0 mm in diameter consisting of a very large number of much smaller microgels. The microgels are themselves very porous and have a spherical shape with a typical diameter of <100 nm. Due to this configuration, macroporous resin beads have two types of internal structure, macroporous and microporous. It is in the pores of the microgels that the active sites of the resin are located. Diffusion of a species to the active site on the resin, therefore, must first diffuse into the macropores, then the micropores before finally interacting with the resin. [1]

2.1.1 Adsorption isotherms

For ion-exchange resins the adsorption isotherm is an important property to understand. The adsorption isotherm is the relationship between the amount of adsorbed species (q) on the adsorbent and the concentration of the fluid phase (c) in equilibrium at a certain temperature. *Equation 1*.

$$q = q(C) \ \ at\ T \quad \text{(Equation 1)}$$

There are a wide variety of different expressions of the kinetics of ion-exchange resins. A popular model for adsorption kinetics is the Langmuir adsorption isotherm model. In this model, the desorption and adsorption are reversible processes and the adsorbate behaves as an ideal gas at isothermal conditions. The reaction of adsorption is shown below where A_g is an empty site, S is the adsorbate and A_{ad} is an occupied site. K_{eq} is the equilibrium constant of the reaction.

$$A_g + S \overset{k_1}{\leftrightarrow} A_{ad} \quad \text{(Reaction 2)}$$

where:

$$K_{eq} = \frac{k_1}{k_{-1}} \quad \text{(Equation 2)}$$

Using the assumptions stated above, the Langmuir adsorption isotherm model can be further derived as:

$$\theta_A = \frac{q_A}{q_{max}} = \frac{K^A_{eq} p_A}{1 + K^A_{eq} p_A} \quad \text{(Equation 3)}$$

Where Θ is the fractional occupancy of the adsorption sites, q_A is the sites occupied by species A, q_{max} is the total number of sites available on the resin, K_{eq} is the equilibrium pressure and p_A is the partial pressure of A in the gas phase. The equation shows the Langmuir adsorption model for the adsorption of a gaseous species A on a homogenous solid surface adsorbent. [2]

Even though the Langmuir adsorption model was derived for gas-phase interactions, it can also be used for liquid-phase adsorption modelling using the equation below.

$$\theta = \frac{q_A}{q_{max}} = \frac{K^A_{eq} C_A}{1 + K^A_{eq} C_A} \quad \text{(Equation 4)}$$

Where C_A is the concentration of species A in the fluid. [3]

In the Langmuir adsorption model, several assumptions are made. The surface of the adsorbent is homogenous, adsorbate molecules do not interact with each other in neighbouring sites, each site can hold at most one molecule and all sites are equivalent. All these assumptions must be considered when modelling the system to obtain valid results. [4] In the case of using the Langmuir adsorption model for ion-exchange

processes using resins, some assumptions fit better than others. The surface of the resin is by no means homogenous due to its macro- and microporous structure. The sites in the resin are equivalent and can hold at most one molecule per site which fits the model well. The interactions between ions in neighbouring sites are assumed to be negligible.

2.2 Mass transfer in ion-exchange processes

Mass transfer is a central topic to consider in ion-exchange purification. Often the desorption/adsorption of species to the resin is very fast relative to the mass transfer of the ionic species to and from the active sites in the resin. Mass transfer is, therefore, the rate-limiting step in most cases of ion-exchange purification. When studying mass transfer in ion-exchange columns, two types of mass transfer are considered, internal and external mass transfer. The overall mass transfer process taking place in the resin consists of the following steps:

1. A counterion (A+) to be removed from the solvent diffuses from the bulk of the solution to the film layer of the solid particle.
2. The counterion (A+) diffuses across the film layer and on to the resin surface.
3. Intraparticle diffusion occurs where the counterion (A+) diffuses into the particle to one of the fixed co-ion sites (R-).
4. The ion previously adsorbed (B+) to the fixed co-ion (R-) desorbs and the counterion (A+) subsequently adsorbs onto the site.
5. Intraparticle diffusion takes place where the desorbed ion (B+) diffuses out of the particle to the particle surface.
6. Further interparticle diffusion of the desorbed ion (B+) from the particle surface to the surface of the film layer before entering the bulk of the fluid.

External mass transfer is the process of mass transfer of a specie from the bulk of the liquid to the surface of the particle. The particle being an ion-exchange resin in this case and the ionic species is the species in question. Internal mass transfer is the intraparticle diffusion of an ionic species from the surface of a particle (resin in this case), to the active site inside the particle. Both the diffusion to the active site from the particle surface and the diffusion from the active site to the particle surface is considered intraparticle diffusion or internal mass transfer. In the sections below, both internal- and external mass transfer will be covered. See *Figure 2* below for an illustration of internal and external mass transfer. [1]

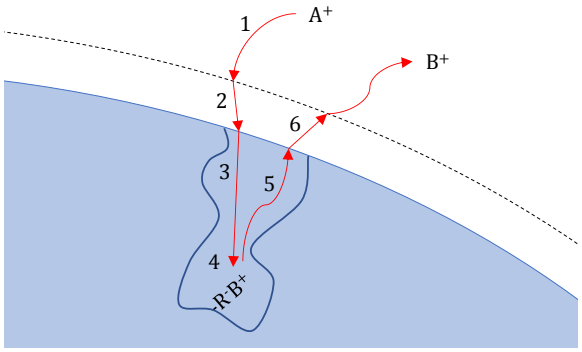

Figure 2: Shows an illustration of mass transfer mechanisms in an ion-exchange process. A+ and B+ are cationic species and R- is the fixed co-ion on the resin.

2.2.1 External mass transfer

When calculating external mass transfer, where species from the bulk diffuse to the surface of the particle, the concept of film diffusion is often used. This model assumes that the concentration of the bulk is uniform and that the resistance to mass transport lies across a thin liquid film in the liquid-solid interface. It is in this

film that the concentration gradient between the solid particle and the bulk liquid is. See *Figure 4* below for an illustration of this film diffusion model. [1]

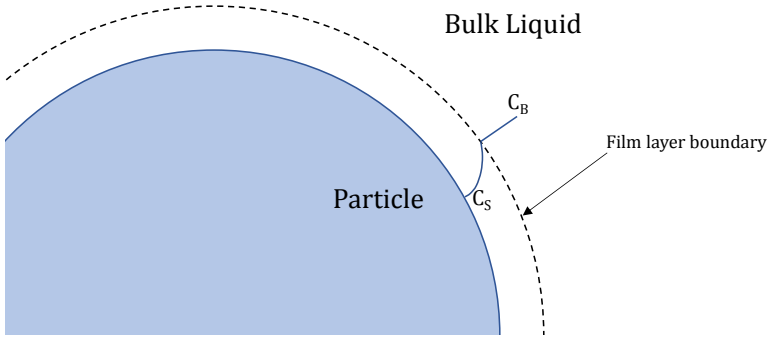

Figure 3: Overview model of film diffusion where the bulk concentration is uniform, and the concentration gradient is shown in the film in the liquid-solid interface. C_B is the bulk concentration and C_S is the surface concentration. The curve shows a decrease in concentration between the film boundary and the particle surface.

During steady-state, where the bulk concentration and the surface concentration is constant, Fick's first law can be used to determine the concentration gradient.

$$J = -D\frac{dC}{dx} \qquad \text{(Equation 5)}$$

Where J is the flux of a species, D is the diffusion coefficient, and dC/dx is the change in concentration with the length of the film layer. As the equation is presented now, the equation only handles one dimension. For two or more dimensions, the following equation is used.

$$J = -D\nabla C \qquad \text{(Equation 6)}$$

Where ∇ is the nabla operator, which denotes the gradient in different dimensions.

Furthermore, by considering the conservation of mass and Fick's first law, Fick's second law can be derived. With Fick's second law, changes in concentration with respect to time as diffusion progress can be calculated.

$$\frac{dC}{dt} = -D\frac{d^2C}{dx^2} \qquad \text{(Equation 7)}$$

Where t is the time, x is the location in space, C is the concentration and D is the diffusion coefficient. [5]

2.2.2 The diffusion coefficient

The diffusion coefficient is, as shown above in Fick's first diffusion law, a proportionality constant between the molar flux J and the concentration gradient. The diffusivity of an ionic species is dependent on the properties of the solvent such as the temperature, viscosity and atomic radius of the species. The diffusion coefficient can be estimated for an ion in a solvent by using the Stokes- Einstein equation as shown below.

$$D_i = \frac{k_B T}{6\pi\mu r_i} \qquad \text{(Equation 8)}$$

Where D_i is the diffusivity of ionic species i, k_B is Boltzmann's constant, T is the absolute temperature, μ is the dynamic viscosity of the solvent and r_i is the effective ionic radius of species i. [6]

2.2.3 Internal mass transfer

As mentioned previously, internal mass transfer is the mass transfer of a species from the particle surface to the active site inside to pores of the particle and analogously the mass transfer of a species from the active site to the surface of the particle. Previously mentioned was also the fact that in most cases, mass transfer is the rate-limiting step for ion-exchange processes. Among the two types of mass transfer, internal and external, internal mass transfer is the slowest of the two in a majority of cases. This gives that very often, internal mass transfer or intraparticle diffusion is the overall rate-limiting step for ion-exchange processes.[1]

Internal mass transfer of a resin particle can be adequately modelled by using Fick diffusion. The diffusive flux inside the pores of the particle can be expressed in the equation below.

$$J_p = \varepsilon_p D_p \frac{dC}{dr} \qquad \text{(Equation 9)}$$

Where J_p is the diffusive flux in the pores, ε_p is the porosity of the particle and D_p is the diffusivity inside the particle pores. The diffusivity inside the pores differs from the diffusivity on the outside of the particle in the bulk fluid. The internal diffusivity (D_p) can, however, be estimated using the external diffusivity (D) and the tortuosity (τ) of the pores. See equation 10 and 11 below. [7, 8]

$$D_p = \frac{D}{\tau} \qquad \text{(Equation 10)}$$

Where

$$\tau = \varepsilon_p + 1.5(1 - \varepsilon_p) \qquad \text{(Equation 11)}$$

There are many models for estimating tortuosity in porous media. Determining the true tortuosity of a sample, however, requires a specific in-depth analysis of the pore structure. In this study, the tortuosity will be calculated using the model developed by Suzuki & Smith 1972. [7]

2.3 Process scaling

To successfully scale up or down a process and ensure the general behaviour of the process stays constant is not as simple as just making the column bigger or smaller. When scaling an ion-exchange adsorption column, certain parameters must be constant between the processes and certain parameters can be changed with more degrees of freedom.

In this case, a large setup is to be scaled down to a lab-scale setup but still allow to predict the same results as the large setup. As mentioned previously, the external mass transfer to and from resin particles depends heavily on the properties of the fluid flow. Among these properties are the viscosity of the fluid, the linear flow velocity and the temperature. The internal mass transfer, however, in addition to previously mentioned parameters, depended heavily on the particle diameter and it is therefore important to ensure that particle dimensions are equal between the processes as well as the properties of the fluid.

To ensure the behaviour of the lab-scale setup is comparable to the large setup, both external and internal mass transfer conditions must be equal to that of the large setup. This means that it must be run with a fluid of equal composition i.e. sucrose concentration, ionic content, temperature, and linear flow. In addition to this, the particle dimensions must be equal between the columns. The recreation of these properties on a lab-scale will not pose any problem. Concentrations and temperatures of the fluid are easily recreated, the fluid velocity is recreated by simple calculations on what volumetric flow is needed at that scale, and the resin properties are made constant by using the same resin in between the processes. There is, however, one more parameter that must be considered, which is the phenomenon in chromatography called the wall effect, which will be discussed below.

2.3.1 The wall effect

To achieve a uniform linear velocity through the column packing in the radial direction, the packing needs to be even so that the void is equal in the radial direction. For a packed bed of spherical particles in a cylindrical column, the void is considerably larger at the interface between the wall and the packing than that of the packing itself. This difference in the void of the packing in radial direction gives rise to the phenomenon called the wall effect. The wall effect in practice gives uneven fluid flow at the column walls compared to that in the centre of the packing, which amplifies dispersion effects in the column effluent. In columns where the ratio of column diameter to particle diameter is large, the wall effects can be assumed negligible as void differences at the wall compared to the packing is very small. At small ratios however, the void at the wall can be much larger in relation to the packing which and cannot be ignored. [9]

In large scale applications the wall effects can often be ignored as a typical column can have a column diameter to particle diameter of 1000:1 typically. At lab-scale however, careful design of the column must be made to ensure wall effects do not dominate. Several studies have been made on this subject with varying ratios for minimum column diameter to particle ratios. A general rule of thumb is to have at least 20:1 ratio but there are sources that say that a ratio of 10:1 is adequate too. Arbuckle & Yen-Fu studied wall effects of a liquid chromatography system for removing volatile organic carbons using activated charcoal. The column to particle diameter ratios examined was 37:1, 22:1, 12.5:1 and 7:1. Arbuckle & Yen-Fu found that column to particle diameter ratios of as low as 7:1 could be used with negligible wall effects. [10, 11]

2.3.2 Dimensionless numbers

As mentioned previously, it is important to keep certain parameters constant between processes when making a large scale or small scale version of a process if it is to behave similarly. For this purpose, dimensionless numbers are often used. Dimensionless numbers used in engineering are expressions that relate certain properties of the system to each other. The number is then used to describe the system more efficiently on a universal basis. Maybe the most famous of dimensionless quantities are Reynolds number as shown below.

$$Re = \frac{\rho v L}{\mu} \qquad \text{(Equation 12)}$$

Where ρ is the density of the fluid, υ is the velocity of the fluid, μ is the dynamic viscosity, and L is the characteristic length. The characteristic length depends on what type of system is observed. In pipes, the characteristic length is the pipe diameter, but across spherical particles it is the particle diameter of the packing. [12]

Another dimensionless number that is relevant for studying transport phenomena is the Péclet number. The Péclet number is a relation between the convective transport rate and diffusive transport rate, *Equation 13*.

$$Pe = \frac{Lv}{D} \qquad \text{(Equation 13)}$$

Where L once again is the characteristic length, υ is the fluid flow velocity and D is the diffusion constant. [13]

For fluid flow through packed beds however, correlations between the Péclet number and Reynolds number has been made. The following equation by Chung and Wen can be used for fluid flows of low Reynolds number in packed, porous beds.

$$Pe = \frac{1}{\varepsilon_b}(0.2 + 0.11 Re_p^{0.48}) \qquad \text{(Equation 14)}$$

Where ε_b is the porosity of the bed and Re_p is the Reynolds number for the column calculated with respect to the particle diameter. Using this equation, the Péclet number can be calculated to have a better understanding

of the dispersion throughout the column. [14] Using the Peclét number, the axial dispersion coefficient is estimated, *Equation 15.*

$$D_{Ax} = \frac{d_p v_{sup}}{Pe_p} \qquad \text{(Equation 15)}$$

Where d_p is the particle diameter, Pe_p is the particle Peclét number and D_{Ax} is the axial dispersion coefficient. [15]

The final dimensionless number to mention is the Schmidt number. The Schmidt number is a relation between viscous diffusion rate and molecular diffusion rate and is used further on to model the mass transfer in the system more easily. The Schmidt number correlation is shown in *Equation 16* below.

$$Sc = \frac{\mu}{\rho D} \qquad \text{(Equation 16)}$$

Where μ is the viscosity of the liquid, ρ is the density of the liquid and D is the Diffusion coefficient for the ionic specie in question. [16]

To simplify the modelling of mass transfer in chromatography systems, efforts have been made to correlate dimensionless numbers of the system and the mass transfer coefficient to predict the mass transfer of a certain species in a system. This was done by Williamson et al who derived the following equation.

$$k_{mass} = \frac{2.4 v_{sup}}{Sc^{0.58} Re_p^{0.66}} \qquad \text{(Equation 16)}$$

Where v_{sup} is the superficial velocity, Sc is the Schmidt number and Re is the particle Reynolds number. With this equation, it is possible to approximate the mass transfer coefficient for a chromatographic separation system. [17]

3 Method

The method is divided into two sections, the first describing the modelling of the process and the second describing the batch experiments for determining the equilibrium isotherm of the resin as well as the column experiments for studying the dynamics of the chromatography process. Complementary information to both the modelling and the experimental setup can be found in the appendix, showing the model code and detailed experimental setups.

3.1 Modelling

Modelling an adsorption column can vary greatly in complexity depending on the degree of detail the user prefers. Ideally, the model should produce as reliable results as possible, mimicking that of an existing setup. In this study, a theoretical model will be made using MATLAB that will be refined to reproduce results made from the lab-scale setup. Empirical models will also be performed, where empirical data measured from the existing lab-scale model will be used to develop a mathematical correlation between process parameters and process performance.

3.1.1 Model structure

This section provides a general overview of the model for the column. Below is a schematic figure of the model structure showing the sequence of events and paths of information.

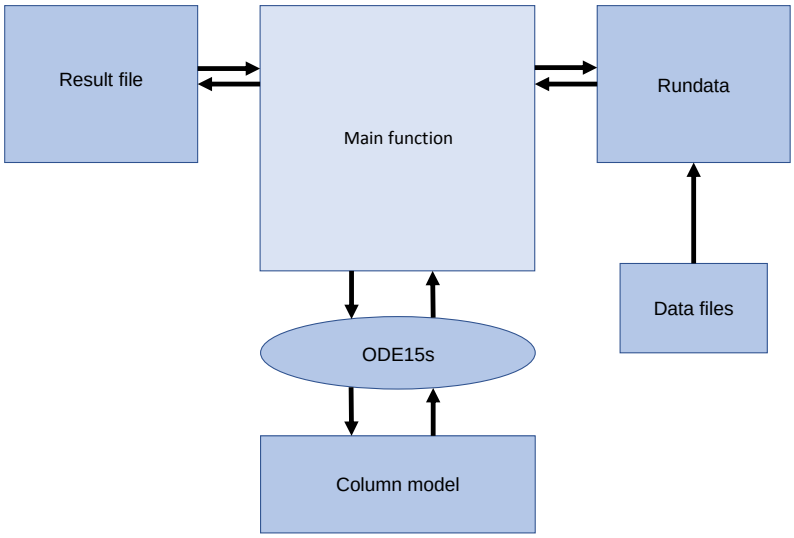

Figure 4: Shows an overview of the model and how information is processed.

The way the model is set up is that the user enters what information they want in the results file. This can be that the user wants to see the breakthrough curve of the model compared to experimental results at a specific glucose concentration for example. The results file sends in the parameters to the main function. The main function is the core of the model that both gathers and distributes data as needed. First the main function requests specific run data and parameters used in experiments to use as input values for the model later. The rundata file, therefore, gathers data from local memory and processes is before sending it to the main function. With all the required information, the main function can now simulate the column using an ordinary differential equation solve (ODE). The ODE receives input from the main function which is passed over to the column model. The column model file contains differential equations that describe the mass balance throughout the system and outputs equation systems for the ODE solver to calculate. The results from the ODE is sent back to the main function, which further sends it to the result file where the data is presented in graphs and figures.

3.1.2 Dynamics modelling

The modelling of chromatography dynamics is a well investigated area of process simulation. In the model presented above, the dynamics are described in the column model section of the complete model. It is in this section that the expressions for the mass transfer and reaction kinetics are described.

The model starts with dividing the length of the column into 50 gridpoints. Each gridpoint can be viewed as if it were a continuously stirred tank reactor (CSTR) with constant inflow and outflow. In each gridpoint, the concentration of ionic species in the liquid and in the resin is calculated using mass balance equations. The general mass balance can be shown as the following expression.

$$0 = \text{IN} - \text{OUT} + \text{PROD} - \text{ACC} \qquad \text{(Equation 18)}$$

Since mass is not created or destroyed in this process, the principle of conservation of mass can be used as shown in the expression above. In this chromatographic process, ionic species enter the system through the inflow (IN), are adsorbed to the resin (ACC) and what is not adsorbed exit the system through the outflow (OUT). No reaction occurs where more ionic species are created, therefore, the production term is assumed to be 0. The mass balance for a gridpoint in the model is thus shown below.

$$0 = \text{IN} - \text{OUT} - \text{ACC} \qquad \text{(Equation 19)}$$

From this basic understanding of the mass balance in each gridpoint, the following equation is derived to express the mass balance for the system mathematically.

$$\frac{dC}{dt} = \frac{-v_{sup}}{\varepsilon}\frac{dC}{dz} + D_{Ax}\frac{d^2C}{dz^2} - \frac{1-\varepsilon}{\varepsilon}\frac{dq}{dt} \qquad \text{(Equation 20)}$$

Where v_{sup} is the superficial velocity, ε is the bed porosity, and D_{Ax} is the axial dispersion coefficient. The first term accounts for the mass transfer via the fluid flow, both in and out, the second term accounts for axial dispersion, and the third term accounts for the accumulation of ionic species in the resin. Furthermore, the accumulation of ionic species in the resin is determined by the isotherm, shown in the equations below.

$$\frac{dq}{dt} = k_{mass}(q_L - q) \qquad \text{(Equation 21)}$$

Where:

$$q_L = \frac{q_{max}K_{eq}C}{1 + K_{eq}C} \qquad \text{(Equation 22)}$$

In equations x above, k_{mass} is the overall mass transfer coefficient, q_L is the Langmuir adsorption and q is the current concentration of adsorbed species in the resin. The Langmuir adsorption q_L is the maximum adsorption capacity of the resin at a certain liquid concentration of ionic species, therefore, the driving force for adsorption in this model is the difference between the maximum adsorption given by the Langmuir equation and the current adsorption concentration q. Equation y above shows the Langmuir adsorption where K_{eq} is the equilibrium constant, q_{max} is the maximum adsorption and C is the liquid concentration of ionic species. See *appendix A1* for the main function of the Matlab code describing the dynamics of the system.

3.2 batch and column experiments

The experiments carried out can be categorized into two different groups, batch experiments and column experiments. The batch experiments are experiments where the equilibrium isotherm of the resin was determined at a specific temperature. The column experiments were experiments where the lab-scale column setup was used to study the behaviour of the resin and the setup in a chromatographic process. The method for both experiments will be explained in separate sections below.

3.2.1 The batch experiments

The objective of the batch experiments was, as mentioned previously, to determine the equilibrium isotherm of the resin. Due to the interest in investigating the column performance at different temperatures and at different concentrations of glucose, the isotherm was determined for the resin at varying temperatures and glucose concentrations. The range of glucose concentrations for which the isotherm was tested was 0, 10, 30 and 50 wt% glucose in water respectively and the range of temperatures were 65, 75, 85 degrees C. All batch experiments were carried out identically with the same equipment disregarding the effect of human error between experiments.

The batch experiments were carried out by putting samples to stir in a water bath at the desired temperature to react until equilibrium. To each sample, a known amount of resin was added, as well as liquid with a known KCl concentration. When equilibrium had been reached, liquid was taken from each sample to analyse the ionic content still in the liquid. With the measured ion concentration, the amount adsorbed to the resin would be calculated and thus the equilibrium isotherm. See *appendix A2* for a detailed description of the experimental setup and execution.

3.2.2 Column experiments

The objective of the column experiments was to study the behaviour of the chromatographic process and the effect of changing certain parameters on the performance of the process. The parameters studied were glucose concentration of feed, feed flow speed and temperature. The glucose concentration was varied by preparing feed solutions of 0, 10, 30, and 50 wt% glucose respectively and pumping them through the setup. The flow speed was varied with the peristaltic pump used and the temperature was varied with the heating element submerged in the water bath.

The column experiments were carried out by first preparing a packed column with a bed thickness of 5 cm resin. Directly above this resin bed, a bed of approximately 5 cm of glass bead is prepared to distribute the flow before entering the resin bed. The packed column is then submerged in a waterbath at a desired temperature before rinsing the column. In the rinsing step, 500 ml of milliQ water is pumped through the system by a peristaltic pump. After rinsing, the prepared feed solution is pumped through, and samples are taken regularly. See *appendix A3* for a detailed description of the experimental setup and execution.

4 Results and discussion

The results will cover two sections, one discussing the batch experiment results and one discussing the column experiments results and the similarity between the model and the experimental data. The main focus will be on the column experiments, and the model since the purpose of the batch experiments was to give data to be used in modelling the process.

4.1 The batch experiments

In the batch experiments the equilibrium isotherm of the resin was studied at 0, 10, 30 and 50 wt% glucose at 75 °C. The objective was to study if the glucose concentration of the liquid had any effect on the isotherm. The temperature effect on the isotherm was also studied. The temperature span studied was 65, 75 and 85 °C for glucose concentrations of 0, 30, and 50 wt% respectively.

4.1.1 Glucose concentration isotherm effect

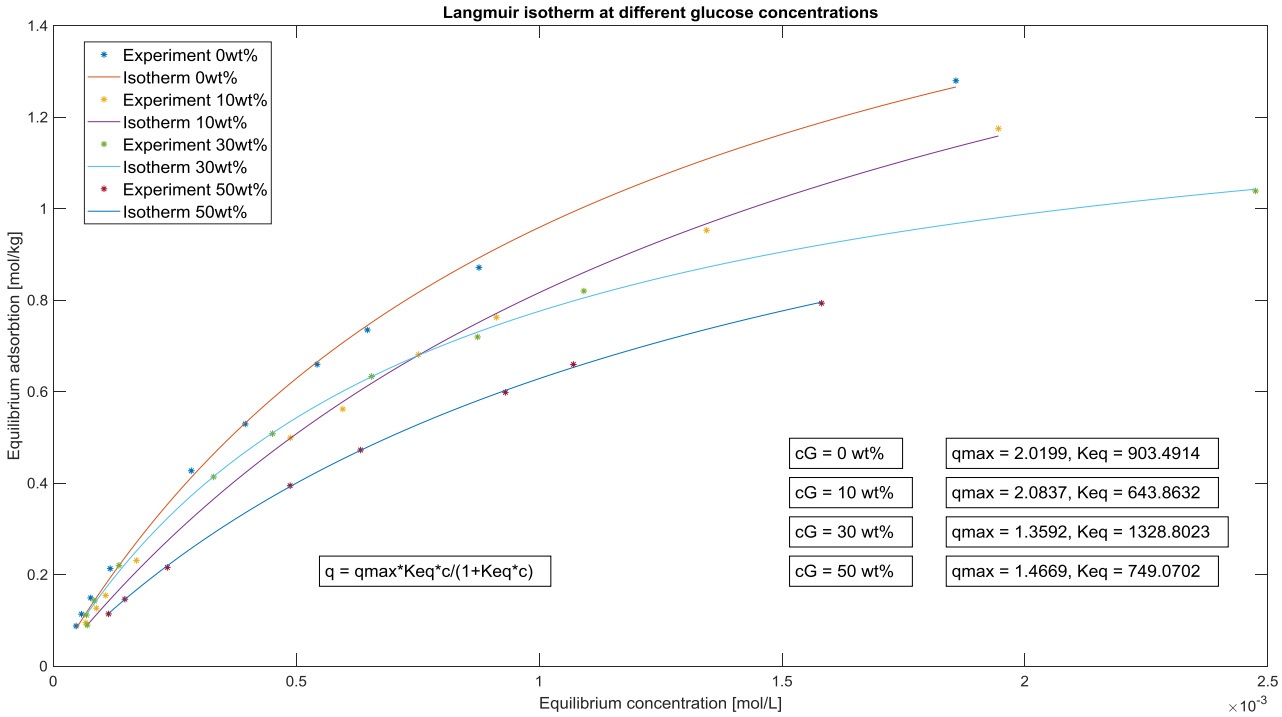

Figure 5: Shows the equilibrium isotherm at 0, 10, 30, and 50 wt% glucose at 75 C. The x-axis is the liquid concentration of K+, and y-axis is the concentration of K+ on the resin.

Initially, the resin adsorption capacity was not expected to decrease with increasing glucose concentration. The results, however, indicates that the adsorption capacity decreases with increasing glucose concentration. This may be an effect of glucose physically blocking sites or entire pores in the resin resulting in decreased resin capacity or possibly that due to the higher viscosity of the liquid, the mass transfer rate in the resin pores is so low that some sites on the resin are not reached within a reasonable amount of time. This has not been investigated in this report. Performing an experiment to see if this is the case in encouraged.

Due to this loss in resin capacity at higher glucose concentrations, there is an argument to be made about the optimal glucose concentration to run the column at from an economic standpoint. To minimize the use of water, which is an expense, the column is preferably run at high glucose concentrations. Running the column at higher glucose concentrations, however, reduces the resin capacity and reduces the time before the need for regeneration between runs. Performing an economic analysis on the subject may prove to be useful.

4.1.2 Isotherm temperature effect

As mentioned previously, the temperature effect on the adsorption isotherm was also studied. The isotherm was studied for 0, 30, and 50 wt% glucose at temperatures 65, 75, and 85 °C. The figures below shows the results.

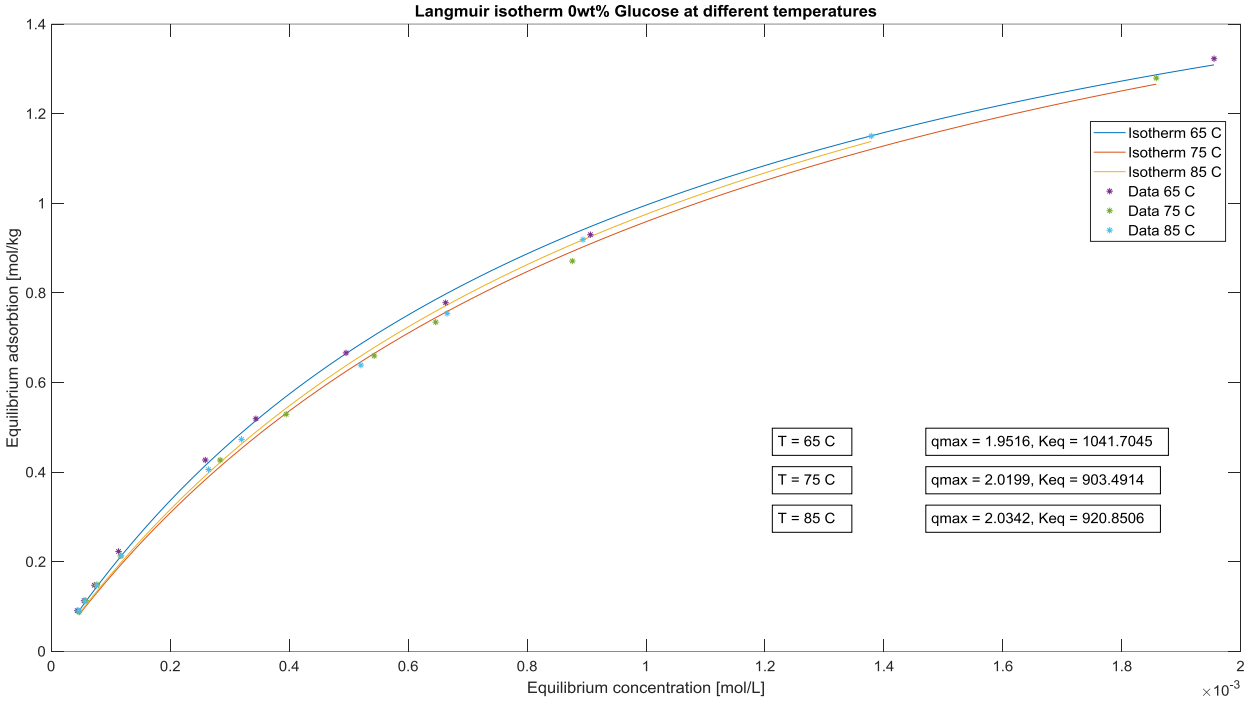

Figure 6: Shows the temperature effect on the equilibrium isotherm at 0 wt% glucose. The markers (*) are the measurement points and the lines are the fitted Langmuir equation for the measurements.

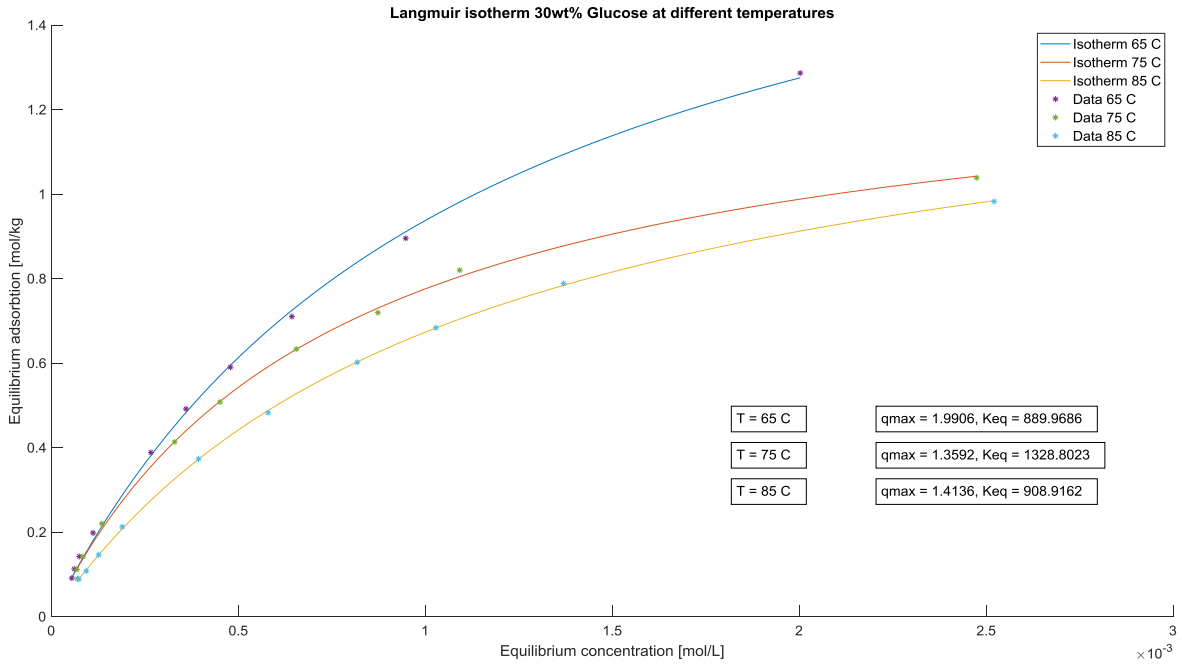

Figure 7: Shows the temperature effect on the equilibrium isotherm at 30 wt% glucose. The markers (*) are the measurement points and the lines are the fitted Langmuir equation for the measurements

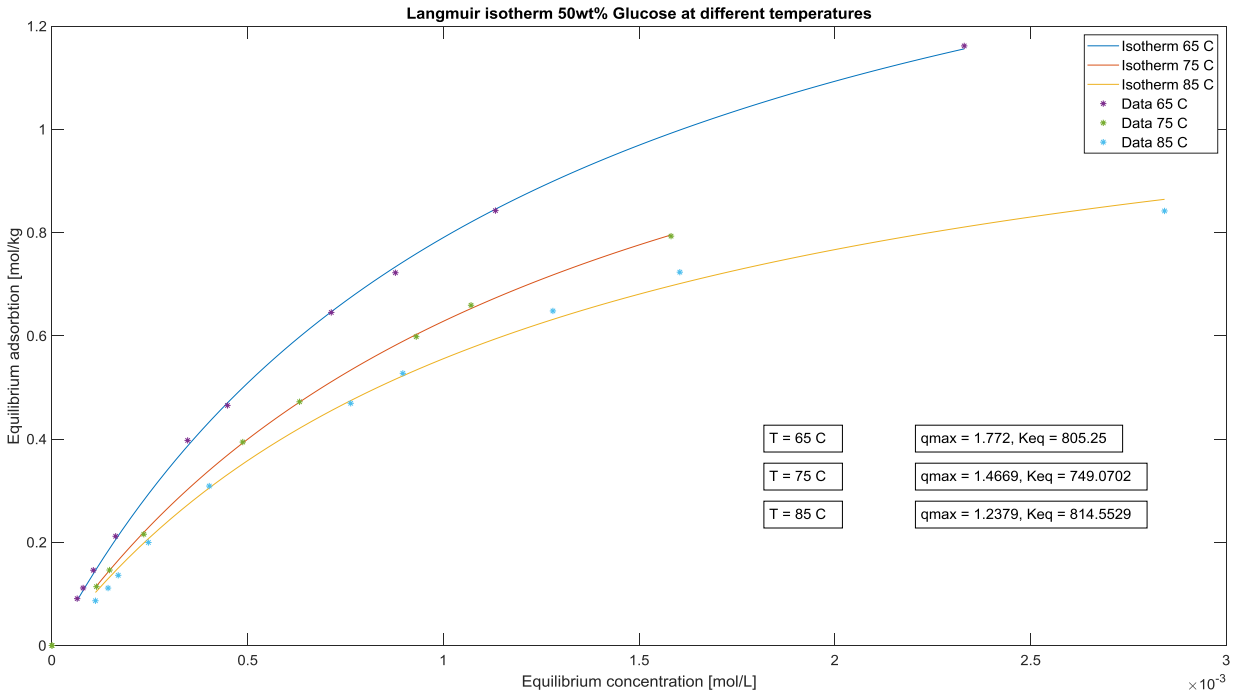

Figure 8: Shows the temperature effect on the equilibrium isotherm at 50 wt% glucose. The markers (*) are the measurement points and the lines are the fitted Langmuir equation for the measurements

As can be seen in the figures above, the temperature has an effect on the equilibrium isotherm of the resin. For 0 wt% glucose, the effect is minimal, and an argument can be made that the difference is no larger than the measurement uncertainty. Moving on to figures 7 and 8, the temperature effect is more pronounced. The trend seems to be that the adsorption of ionic species to the resin is more favoured at lower temperatures, allowing the equilibrium to settle at lower concentrations of ionic species in the liquid. For both 30 and 50 wt% glucose, this same behaviour is observed. The trend of higher adsorption at lower temperatures may be explained by the adsorption reaction being slightly exothermic, in which case the decrease in temperature would favour the adsorption reaction in accordance with Le Chatelier's principle.

The higher equilibrium adsorption at lower temperatures indicates that the process could be run more economically at lower temperatures with respect to running time before saturation of the column. In practice however, the lower temperature also influences the mass transfer rate in the liquid. At high viscosities, i.e. high glucose concentrations, the mass transfer rate is reduced significantly with temperature and the most viable option may be to run the column at higher temperatures to increase the mass transfer rate even though the resin has a lower capacity.

4.2 Column experiments

For the column experiments, two parameters were varied. The first is the concentration of glucose in the feed and the second is the linear flow velocity through the column. The concentration of glucose tested was 0, 10, 30 and 50 wt%. The flow was varied by taking the recommended ideal flow rate given by the manufacturer of the large scale process and then testing double and half the flow rate relative to the ideal. The ideal flow rate was a linear flow velocity of 1.3 m/h, which gives that the half and double flow were 0.65 and 2.6 m/h linear flow velocity, respectively. First the influence of the glucose concentration on the feed will be studied, thereafter the effects of changing the flow velocity. For all results, a comparison between model results and

experimental results will be made. Before presenting the results, a brief discussion on the reproducibility and validity of the results will be given below.

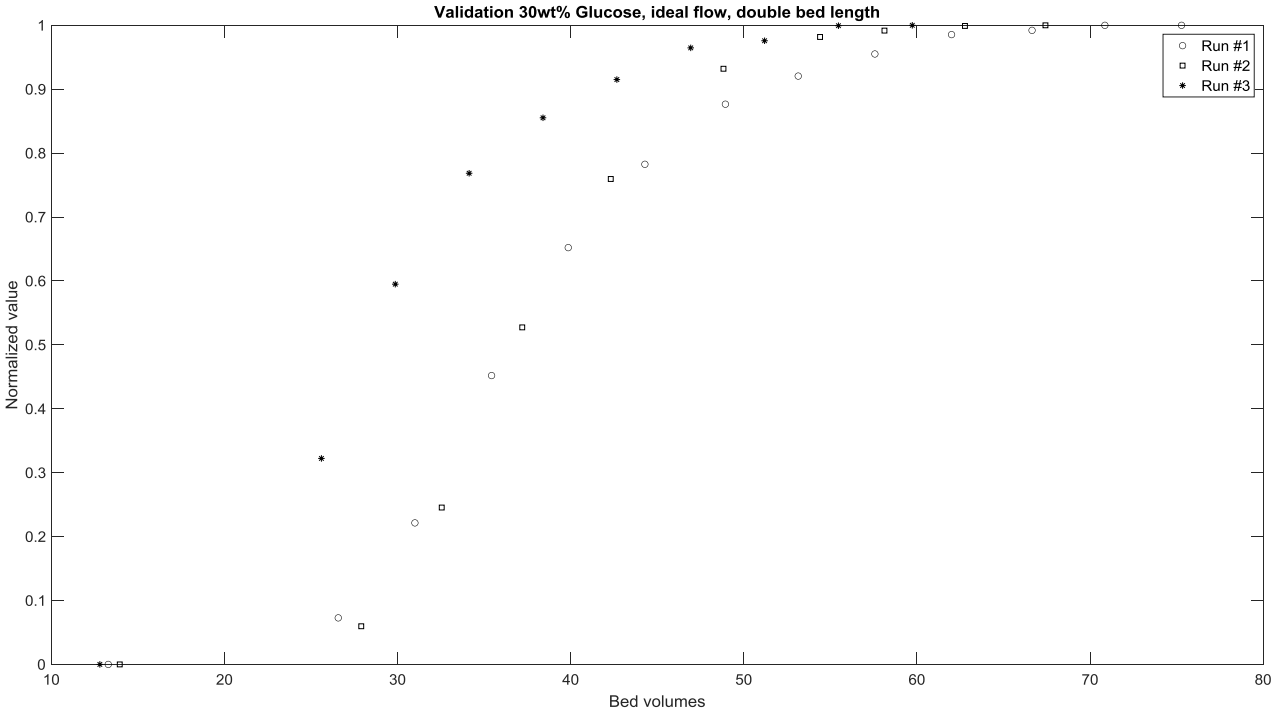

Figure 9: Shows the breakthrough curve for 3 column experiments using 30 wt% glucose and 1,3 m/h linear flow velocity. All three experiments were run at the same conditions at 75 C and with a resin bed thickness of 10 cm.

The figure above shows the results of 3 column experiments run at identical conditions at a temperature of 75 °C, 30 wt% glucose concentration and ideal flow, i.e. a linear flow velocity of 1.3 m/h. As shown in the image, the shape of the breakthrough curve is very similar, but the position of the curve can vary. The early breakthrough of Run #3 shown in the figure may be a cause of the resin not being fully utilized. Channelling might be an issue where portions of the resin bed are not reached by the liquid and therefore the breakthrough comes out earlier than expected. The shape of the breakthroughs is very similar, however, between experiments. This indicates that the shape of the breakthrough curve holds higher credibility, whereas the position of the breakthrough must be held with caution due to the varying results.

4.2.1 Feed glucose effects

The glucose concentrations of the feed studied were 0, 10, 30, and 50 wt% glucose, respectively. All experiments were carried out at the same flow velocity at 1.3 m/h linear flow velocity through the column, at a temperature of 75 °C and a resin bed thickness of 5 cm. All experiments were carried out with the same concentrations of K+ in the feed of 25.7 mmol/L with a reservation for small measurement differences between experiments.

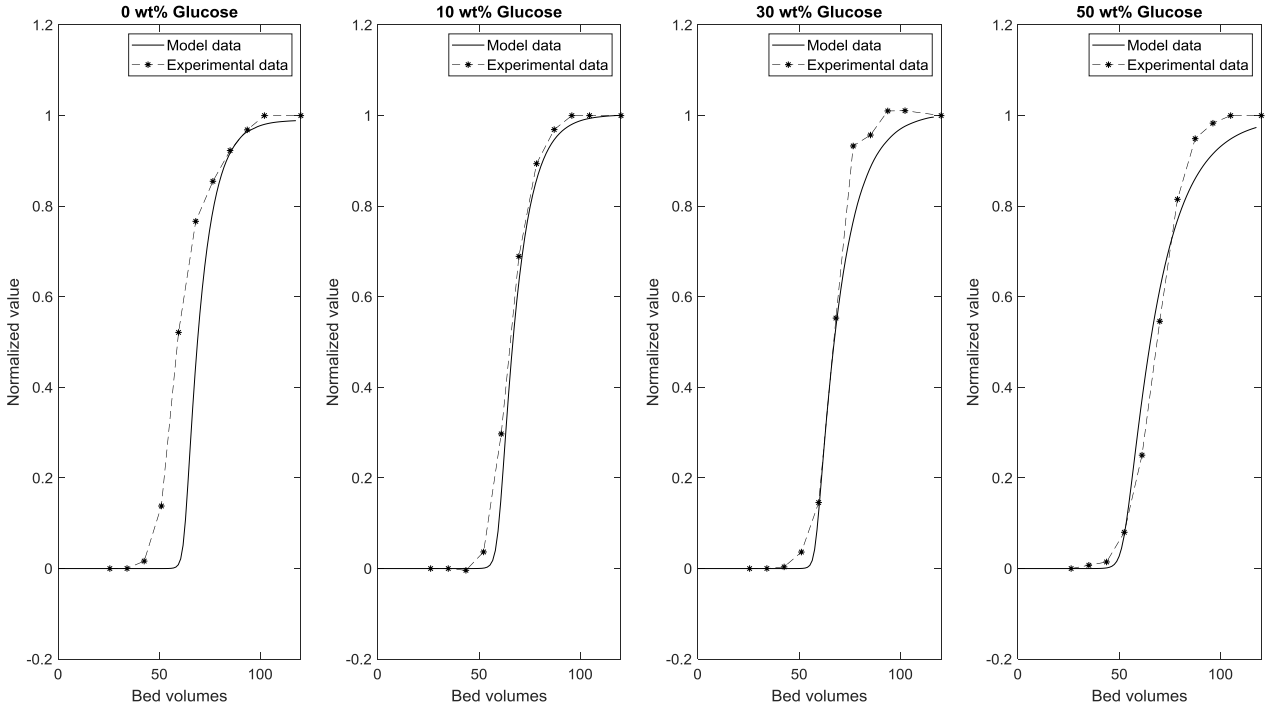

Figure 10: Shows the breakthrough curve of both experimental data and model data for glucose concentration 0, 10 30 and 50 wt% glucose at ideal flow with a resin bed thickness of 5 cm. The solid line depicts the model data and the dashed line the experimental data.

Comparing the breakthrough curves of the model versus experimental data individually in *figure 10* above shows promising results with respect to similarities between the model and experimental data for glucose concentrations 10, 30 and 50 wt%. Experimental data for 0 wt% glucose seem to deviate from the model, however. Irregularities in the packing is suspected to be the issue and repeating of this experiment is encouraged.

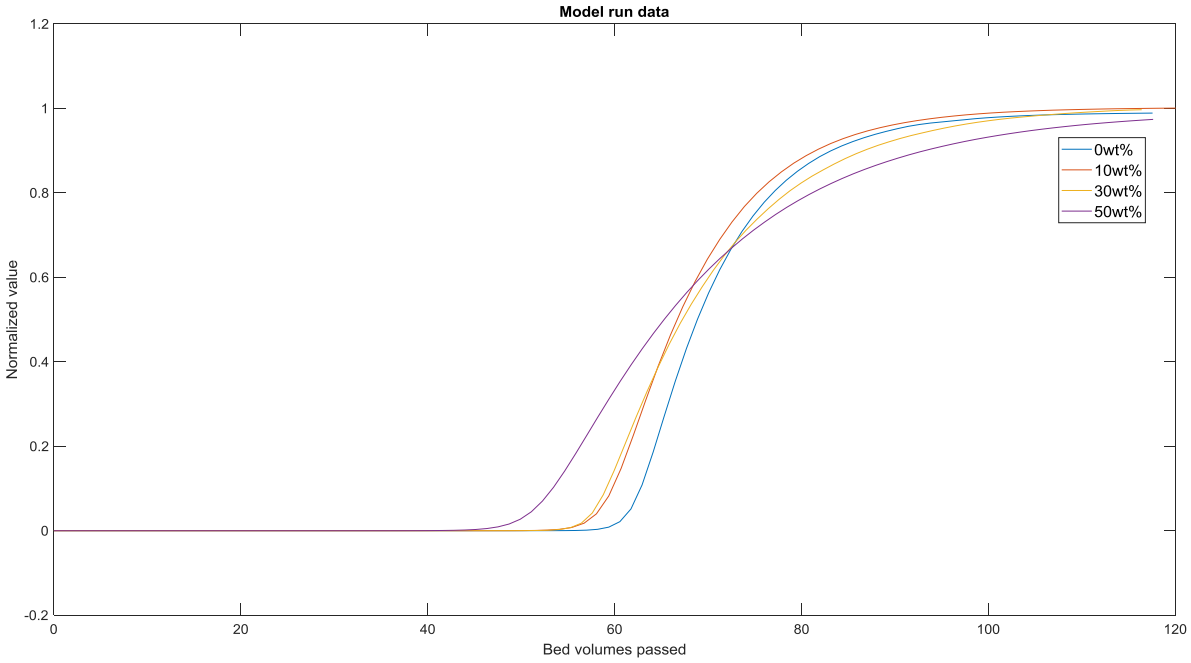

Figure 11: Shows the model results for all glucose concentrations in one figure.

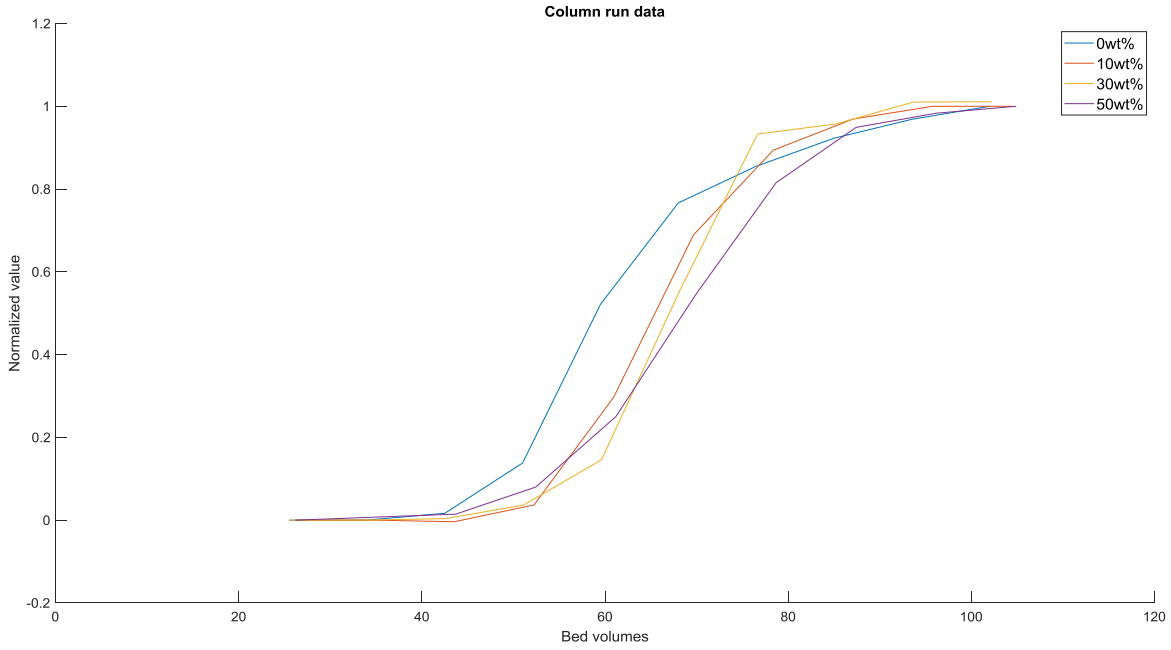

Figure 12: Shows the column experiments results for all glucose concentrations in one figure.

In *figure 10* the breakthrough curves for feed glucose concentrations of 0, 10, 30, and 50 wt% as well as the model results for each concentration can be seen. With higher glucose concentration, the viscosity of the feed

solution increases. What is expected is that the increased viscosity gives slower mass transfer and therefore a flatter breakthrough curve and an overall less efficient process. The model demonstrates this behaviour in *figure 11*. This behaviour can however, not be seen in *figure 12* where experimental data is shown. Early breakthrough, coupled with unexpected breakthrough curve shape for 0 wt% glucose counters the behaviour shown in the model. The breakthrough curves of 10 and 30 wt% glucose are very similar in both model, and experimental data and the breakthrough curve for 50 wt% glucose has the flattest shape, which coincides with what is expected.

4.2.2 Feed flow-rate effects

The effects of feed flow rate were studied by first running the column at normal flow which is at a linear velocity of 1.3 m/h. The linear flow velocity was then halved for another run at the same conditions, and finally, the linear flow velocity was doubled for a third run. This was done for glucose concentrations 0, 10, 30, and 50 wt% at 75 °C with a resin bed thickness of 5 cm.

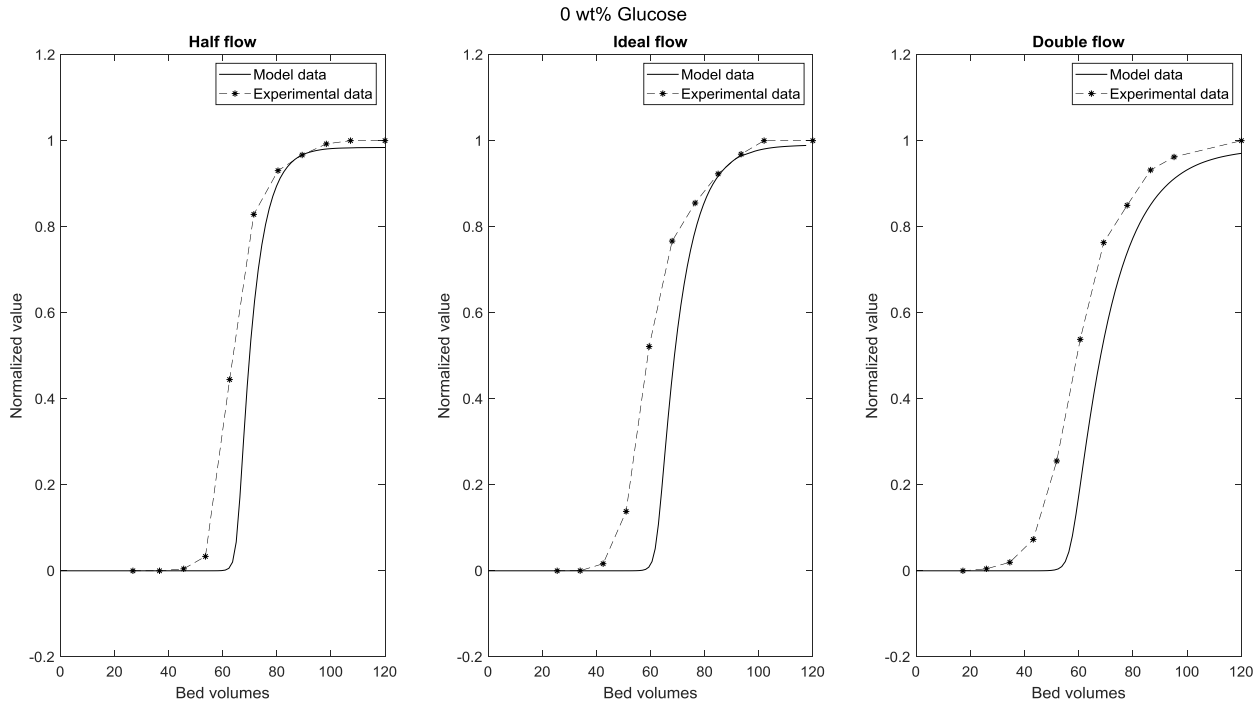

Figure 13: Shows the effect of varying the linear flow velocity on the breakthrough curve for 0 wt% glucose. All tests were carried out at 75 °C, with a bed thickness of 5 cm.

As depicted in *figure 13* above, linear flow velocity has an effect on the shape of the breakthrough curve which is to be expected. The trend seems to be for the experimental data that the breakthrough comes out earlier and the shape of the curve is flatter at higher linear flow velocity. The model also displays the flatter breakthrough at higher linear flow velocity, but the position of the breakthrough curve is only marginally different between experiments.

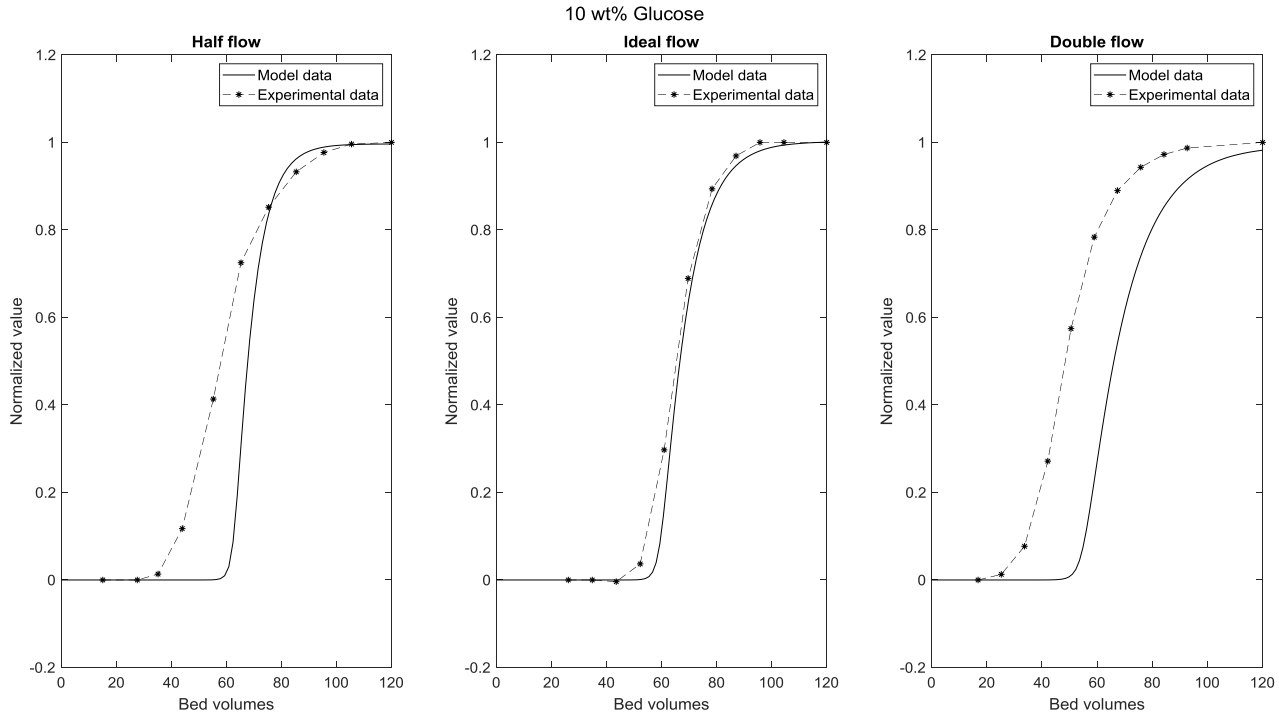

Figure 14: Shows the effect of varying the linear flow velocity on the breakthrough curve for 10 wt% glucose. All tests were carried out at 75 °C, with a bed thickness of 5 cm.

Similarly to *figure 13*, *figure 14* also shows the effects of linear flow velocity on the breakthrough curve with the difference being that the feed liquid fed to the column having a glucose concentration of 10 wt%. The shape of the results is very similar comparing the model and experimental breakthrough curves for both ideal and double flow. The position of the breakthrough curve for ideal flow coincides well with the experimental results, but the same is not observed for double flow. The experimental results once again come out earlier than expected as if portions of the resin are not utilized. The half flow experiment, however, seems to deviate much from what is expected. This may be explained by irregularities in the packing in which case the experiment should be repeated to ascertain if this indeed was the case.

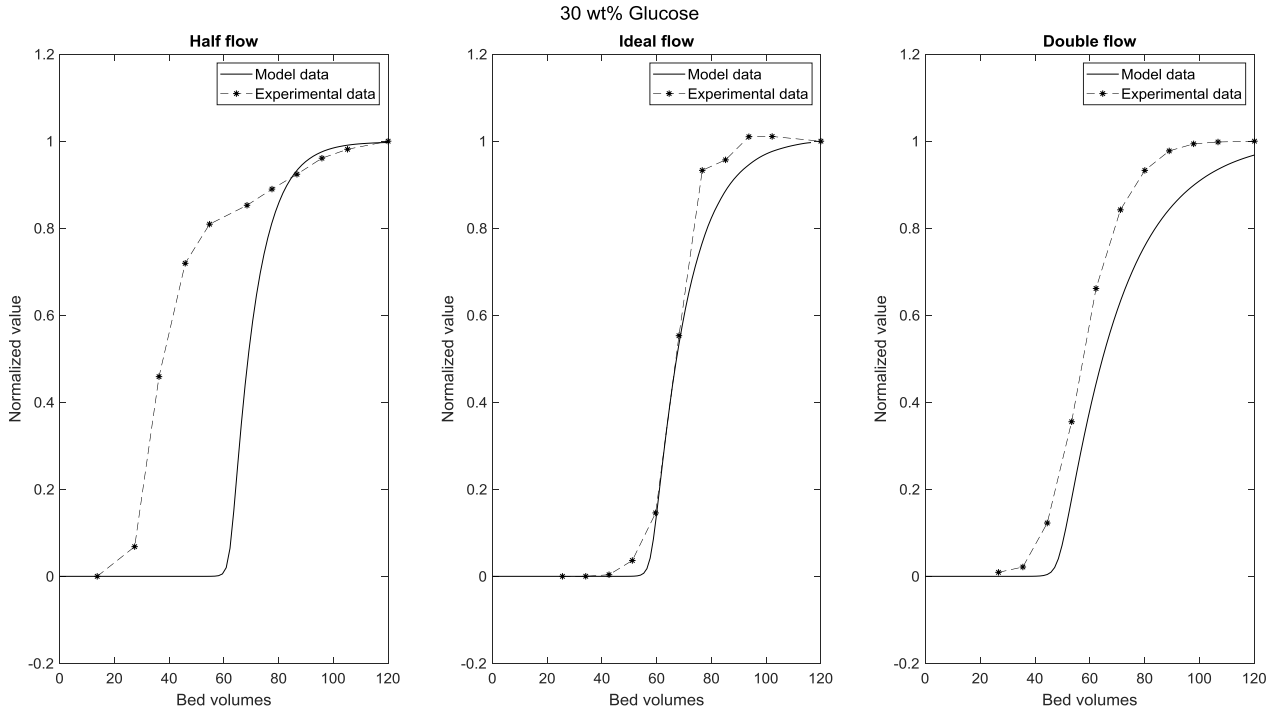

Figure 15: Shows the effect of varying the linear flow velocity on the breakthrough curve for 30 wt% glucose. All tests were carried out at 75 °C, with a bed thickness of 5 cm.

Reviewing the breakthrough curves for varying linear flow velocity for a liquid with 30 wt% glucose, the shape of the breakthrough curves once again is very similar to experimental data for the ideal and double flow. Concerning the position of the breakthrough curve, the model and experimental values for ideal flow are very similar, whereas, for double flow, the position of the breakthrough curve comes out earlier than the model predicts. The half flow experiments deviated once again from expected results and were therefore disregarded.

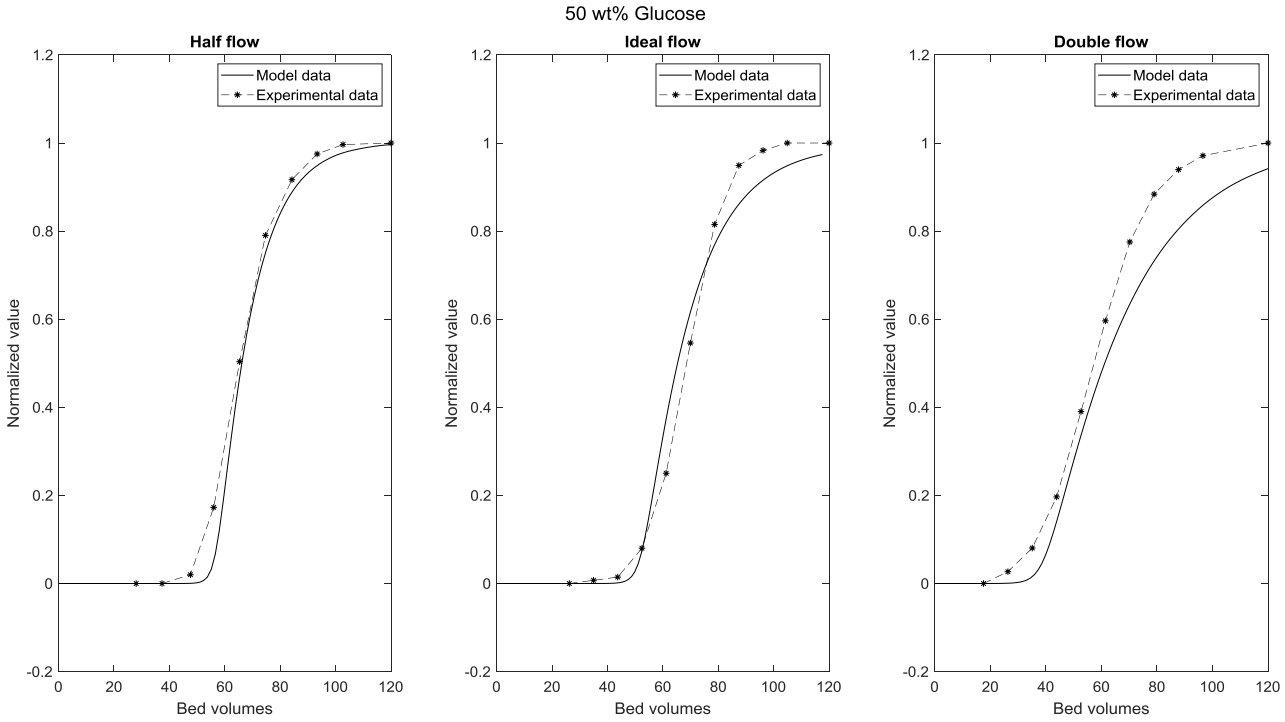

Figure 16: Shows the effect of varying the linear flow velocity on the breakthrough curve for 50 wt% glucose. All tests were carried out at 75 °C, with a bed thickness of 5 cm.

The breakthrough curves for both model and experimental data using a glucose concentration of 50 wt% with varying linear flow velocities are shown in *figure 16* above. Here the shape of the breakthrough curves coincides very well between model data and experimental data for all flows. The position of the breakthrough curves is also very close between model and experimental data for half the flow and the ideal flow. The breakthrough comes out earlier than expected however for the double-flow experiment.

The general trend of the results in *figures 13 to 16* above is that the higher the linear flow velocity is, the flatter the shape of the breakthrough becomes. This behaviour can be seen in both the model data and the experimental data. The position of the breakthrough for the experimental data seems to deviate from what is expected a number of times.

5 Conclusion

The conclusion, as with other parts of the report, will be divided into two sections. One concerning the equilibrium isotherm experiments and one concerning the column experiments and its similarities to the model. After the conclusion, further work is discussed.

From the presented results of this assignment, the goal is considered completed. The goal being to construct a functioning lab-scale unit and model the unit using Matlab to predict results. The question posed in the introduction has also been answered, a lab-scale version can be constructed and operated, and the system can be modelled to predict the behaviour ion exchange of glucose solutions.

5.1 Isotherm experiments

From measuring the equilibrium isotherm with varying glucose concentrations in the liquid, results indicate that higher glucose concentration gives poorer resin performance. If this effect is an effect of the increased viscosity of the liquid, glucose physically blocking sites or entire pores in the resin or a mix of the two is unclear.

The temperature also proved to have a clear effect on the equilibrium isotherm at higher glucose concentrations. The resin proved to have higher adsorption capacity at lower temperatures. A theory of this behaviour was proposed earlier. If the adsorption reaction of ionic species to the resin is slightly exothermic, then lower temperatures would favour the adsorption of ionic species to the resin and push the equilibrium to the right in accordance with Le Chatelier's principle if the adsorption reaction is exothermic, which has not been researched here.

5.2 Column and model experiments

There are examples from the results that show the model can successfully predict the experimental results. Both in position of the breakthrough curve and shape of the breakthrough curve the model and the experimental results have coincided on several experiments. There is however a fair bit of deviating experimental results from what the model predicts and what is expected. At lower fluid velocities, the results from the column experiments often deviated substantially from the model results. The reason for this behaviour has not been determined fully. The simplest explanation for this is irregularities in the packing which gives rise to preferential paths and thus early breakthrough and broader breakthrough curves. If this were the case, however, the poor performance would be observed for all fluid velocities. Lower fluid velocities might amplify the effects of irregular packing on the breakthrough curve, which might be why these deviations in results from what is expected is mostly observed for lower fluid velocities.

5.3 Further work

Originally the plan for this assignment was to study both the effect of linear flow velocity and temperature effect on the process. However, due to a fair amount of failed experiments and loss of time during relocation of equipment, the experiment plan was rescheduled and only the effect of linear flow velocity was studied. With more time the temperature effects would be studied of a temperature range of 65, 75 and 85 C. Since the resin equilibrium isotherm has been studied for the temperature span of 65, 75 and 85 C, the model is equipped with the data needed to simulate the column under such conditions.

Most column experiments performed used a resin bed of 5 cm except for 3 experiments using a 10 cm resin bed. All experiments used a 5 cm glass distribution bed above the resin bed to distribute the flow evenly. Experiments throughout the project showed varying results from what is expected from time to time. With the short resin bed of 5 cm, it is likely that uneven packing gives rise to channelling in the bed which leads to parts of the bed not being utilized and early breakthrough of the column. This issue was observed even after increasing the resin bed thickness to 10 cm. To increase reproducibility for the setup, an approach could be to study the method of packing the column to ensure a more even packing. An option is to pack the column

using a liquid-solid slurry where the packing is mixed with liquid and poured into the column. The bed is then subjected to high flows to pack the bed. Using this method, the bed may be more evenly packed, and reproducibility may increase.

To eliminate the error between experiments of packing a new resin bed each run, an option could be to use the same resin bed multiple time by regenerating the bed once it has been saturated. This method would ensure that the bed remains the same between experiments and could reduce variations in results between experiments. Assuming the resin does not loose capacity between regeneration washings, each experiment should have identical resin bed.

The span of glucose concentrations studied for both isotherm experiments and column experiments was 0, 10, 30, 50 and 70 wt% glucose. For both isotherm experiments and column experiments however, 70 wt% glucose gave poor data. The high amount of glucose seemed to affect the ion selective electrode readings heavily despite theoretically there should not be an effect. The effect of glucose on ion selective electrode results should therefore be studied. For the column experiments, the high viscosity of the feed solution at 70 wt% glucose decreased the mass transfer rate significantly. Due to this decrease in mass transfer, the effluent of the column showed breakthrough very early in the experiments. The resin bed length should be increased from 5 cm for experiments to ensure that the effluent of the column does not show immediate breakthrough due to the low residence time of the column.

References

1. SenGupta, A.K., *Ion Exchange Fundamentals*, in *Ion Exchange in Environmental Processes*. 2017, John Wiley & Sons, Inc. p. 50-129.
2. Hanaor, D.A.H., et al., *Scalable Surface Area Characterization by Electrokinetic Analysis of Complex Anion Adsorption.* Langmuir, 2014. **30**(50): p. 15143-15152.
3. Bankar, A. and G. Nagaraja, *Chapter 18 - Recent Trends in Biosorption of Heavy Metals by Actinobacteria*, in *New and Future Developments in Microbial Biotechnology and Bioengineering*, B.P. Singh, V.K. Gupta, and A.K. Passari, Editors. 2018, Elsevier. p. 257-275.
4. Fichthorn, K.A., *Principles of Adsorption and Reaction on Solid Surfaces. Richard I. Masel.* Journal of Catalysis, 1997. **170**(1): p. 214.
5. Fick, A., *V. On liquid diffusion.* The London, Edinburgh, and Dublin Philosophical Magazine and Journal of Science, 1855. **10**(63): p. 30-39.
6. Pawlowicz, R., *Electrical Properties of Sea Water: Theory and Applications.* Reference Module in Earth Systems and Environmental Sciences, 2015.
7. LeVan, M.D. and G. Carta, *Adsorption and Ion Exchange*. 2008: McGraw-Hill.
8. Suzuki, M. and J.M. Smith, *Dynamics of diffusion and adsorption in a single catalyst pellet.* AIChE Journal, 1972. **18**(2): p. 326-332.
9. Niu, M., et al., *Reduction of the wall effect in a packed bed by a hemispherical lining.* AIChE Journal, 1996. **42**(4): p. 1181-1186.
10. Arbuckle, W.B. and Y.-F. Ho, *Adsorber Column Diameter: Particle Diameter Ratio Requirements.* Research Journal of the Water Pollution Control Federation, 1990. **62**(1): p. 88-90.
11. Önsan, Z.I. and A.K. Avci, *Multiphase Catalytic Reactors: Theory, Design, Manufacturing, and Applications*. 2016: Wiley.
12. Alveteg, M., *Handbook : Physical properties, correlations and equations in chemical engineering*. 2013: Department of Chemical Engineering, Faculty of Engineering.
13. Patankar, S.V., *Numerical heat transfer and fluid flow*. Series in computational methods in mechanics and thermal sciences. 1980: Hemisphere.
14. Atmakidis, T. and E. Kenig, *Numerical Analysis of Residence Time Distribution in Packed Bed Reactors with Irregular Particle Arrangements.* Chemical Product and Process Modeling, 2014. **0**.
15. Rastegar, S.O. and T. Gu, *Empirical correlations for axial dispersion coefficient and Peclet number in fixed-bed columns.* Journal of Chromatography A, 2017. **1490**: p. 133-137.
16. Incropera, F.P. and D.P. DeWitt, *Fundamentals of heat and mass transfer*. 5. ed. ed. 2002: Wiley.
17. Williamson, J., K. Bazaire, and C. Geankoplis, *Liquid-Phase Mass Transfer at Low Reynolds Numbers.* Industrial & Engineering Chemistry Fundamentals, 1963. **2**.

Appendix

A1 Model main function code

```
function dzdt = steelmodel(t,z,p)
    h = p.L/p.N;            %Size of gridpoints

    c = z(1:p.N);           %[g/L]
    q = z(p.N+1:p.N*2);     %[g/L]

    c0 = 2*p.cin-c(1);      %Dirichlet boundary inlet
    cnew = [c0 c'];         %Paste dirichlet to concetrationvector
    cnew2 = [cnew c(end)];  %Add a point to last position in simulation

    dcdz = (cnew2(2:end-1) - cnew2(1:end-2))/h; %Expression for the derivative
using point before and point after
    d2cdz2 = (cnew2(3:end) - 2*cnew2(2:end-1) + cnew2(1:end-2))/h^2; %Expression
for the second derivative using point before, after and central point.

    qL = (p.qmaxL*p.KeqL*c./p.MK)./(1+p.KeqL*c./p.MK); %mol/kg LANGMUI ISO

    %Adsorbtion kinetics. Since adsorbtion reaction is considered instant,
    %the mass transfer to the sites are limiting. Ths is given by the mass
    %transfer coeff kmass.
    rkonst = p.kmass*(qL*p.MK*p.rhores*10^-3-q);
    dqdt = rkonst;
    dcdt = -p.vsup/p.ecc*dcdz + p.Dax*d2cdz2 -(1-p.ec)/p.ec*dqdt';
    dzdt = [dcdt dqdt']';
end
```

A2 Batch experiments equipment and materials

Resin A in its hydrated form
MilliQ water
KCl salt, reagent grade 99.5% pure
D-()-Glucose, Anhydrous 99.5% pure
11 50 ml bluecap bottles
11 magnetic stirrers
1 1000 ml bluecap bottle
1 50 ml measuring cylinder
1 15 sites magnetic stirrer with a water bath
1 Heating unit
1 Metrohm conductivity meter
1 Mettler Toledo PerfetIon K+ electrode

A2.1 Batch experiment method

1. Prepare a 600 ml solution of anhydrous D-()-Glucose and milliQ water of the desired concentration.
2. Add 230 mg of KCl to the solution and stir until fully dissolved.
3. Measure and add increasing amounts of resin A to blue cap bottles 1 to 10. See the table below for the specific amount to add to each bottle.

Bottle no	**1**	**2**	**3**	**4**	**5**	**6**	**7**	**8**	**9**	**10**
Resin [mg]	115	229	286	343	458	572	1144	1716	2288	2860

4. Measure and add a similar amount of resin to the 11th blue cap bottle as was added to bottle 1.
5. Add 50 ml of the previously prepared KCl + glucose solution to bottles 1 to 10 and add magnetic stirrers to each and set the bottles to stir in a water bath at the desired temperature.
6. Add 50 ml of KCl + glucose solution and a magnetic stirrer to the 11th bluecap bottle and put in the conductivity meter electrode to continuously measure the conductivity.
7. Add the 11th bluecap bottle to the water bath and start measuring conductivity. Note down the conductivity every 5 minutes.
8. Let all samples stir in the water bath until the conductivity has stabilized and does not change over the 5 minute span.
9. Remove the bottles and take samples of the liquid. Make sure no resin is in the samples.
10. Measure the remaining K+ concentration of the liquid samples using the K+ selective electrode.

A3 Column experiments equipment and materials

Resin A in its hydrated form
MilliQ water
KCl salt, reagent grade 99.5% pure
D-()-Glucose, Anhydrous 99.5% pure
Glass wool
Glass beads, 2mm diameter
1 heating element with water bath
1 peristaltic pump
1 balance
1 hotplate
1 3000 ml Bluecap bottle
1 1500 ml Bluecap bottle
12 25 ml Bluecap bottles
1 Metrohm conductivity meter
1 Steel column (Length 200mm, Inner diameter 22mm) with inflow and effluent fittings.

A3.1 Column experiments method

1. Prepare a 3000 ml solution of anhydrous D-()-Glucose and milliQ water of the desired concentration. Heat the solution with the hotplate to the desired temperature.
2. Add 5757 mg KCl to the solution and stir until fully dissolved.
3. Measure 15,205 g resin A and 29,2 g of glass beads in separate containers. This gives a 5 cm bed of resin and a 5cm distribution bed of glass beads once added to the column.
4. Put a small amount of glass wool in the bottom of the column to ensure no resin leaks to the effluent.
5. Gently pour in the resin and occasionally tap the column to settle the resin in a close packing.
6. Gently pour in the glass beads using the same method as used for the resin.
7. Seal the column and submerge into water bath.
8. Rinse the column with 500 ml milliQ water using the peristaltic pump. While rinsing, use the scale to ensure that the flow is correct.
9. Start pumping the feed into the column at the desired flow velocity. Make sure the feed is at the desired temperature to avoid a thermal shock of the resin as feed enters.
10. Take samples of the effluent and let cool before measuring with the conductivity meter. Once the conductivity metre value is constant between samples, the bed is fully saturated, and the process can be shut down.